

PISCO2: the new speckle camera of the Nice 76-cm refractor

R. Gili¹, J.-L. Prieur^{2,3,*}, J.-P. Rivet⁴, F. Vakili¹, L. Koechlin^{2,3}
D. Bonneau⁴

¹ UMS 2202, Université de Nice Sophia Antipolis – CNRS
Observatoire de la Côte d’Azur, CS 34229, 06304 Nice Cedex 4, France

² CNRS – IRAP, 14 avenue E. Belin, 31400 Toulouse, France

³ Université de Toulouse – UPS-OMP – IRAP, Toulouse, France

⁴ UMR 7293, Université de Nice Sophia Antipolis – CNRS
Observatoire de la Côte d’Azur, CS 34229, 06304 Nice Cedex 4, France

Received May 28, 2014; accepted

Abstract

We present the new speckle camera PISCO2 made in 2010–2012, for the 76-cm refractor of Côte d’Azur Observatory. It is a focal instrument dedicated to the observation of visual binary stars using high angular resolution speckle interferometry techniques to partly overcome the degradation caused by the atmospheric turbulence. Fitted with an EMCCD detector, PISCO2 allows the acquisition of short exposure images that are processed in real time by our specially designed software. Two Risley prisms are used for correcting the atmospheric dispersion. All optical settings are remotely controlled. We have already been able to observe faint close binary stars with angular separations as small as 0".16, and visual magnitudes of about 16. We also have measured some particularly difficult systems with a magnitude difference between the two components of about 4 mag. Those performances are very promising for the detection and study of large sets of yet unknown (or partly measured) binaries with close separation and/or large magnitude difference.

1 Introduction

This paper presents the new speckle camera PISCO2 (Pupil Interferometry Speckle camera and COronagraph, 2nd version) made in 2010–12 for the 76-cm refractor telescope (“Grand Equatorial de l’Observatoire de la Côte d’Azur”, hereafter L76). PISCO2 is a focal instrument the purpose of which is to provide high angular resolution images using speckle interferometry techniques. Those techniques allow to partly overcome the degradation caused by atmospheric turbulence (Labeyrie, 1970).

PISCO2 is a simplified version of PISCO that was developed in 1993 for the 2-meter Bernard Lyot telescope (Pic du Midi, France). PISCO is a multi-purpose focal instrument with many observing modes: pupil interferometry, pupil-mask aperture synthesis, SCIDAR atmospheric turbulence measurements, grism spectroscopy, coronagraphy, and Shack-Hartmann wavefront sensing. A detailed presentation can be found in Prieur et al. (1998). Since 2004 PISCO has been operated on a dedicated 1-meter telescope in Merate (Brera Observatory, Italy) (see e.g., Scardia et al., 2007, 2013).

*Corresponding author: jean-louis.prieur@irap.omp.eu

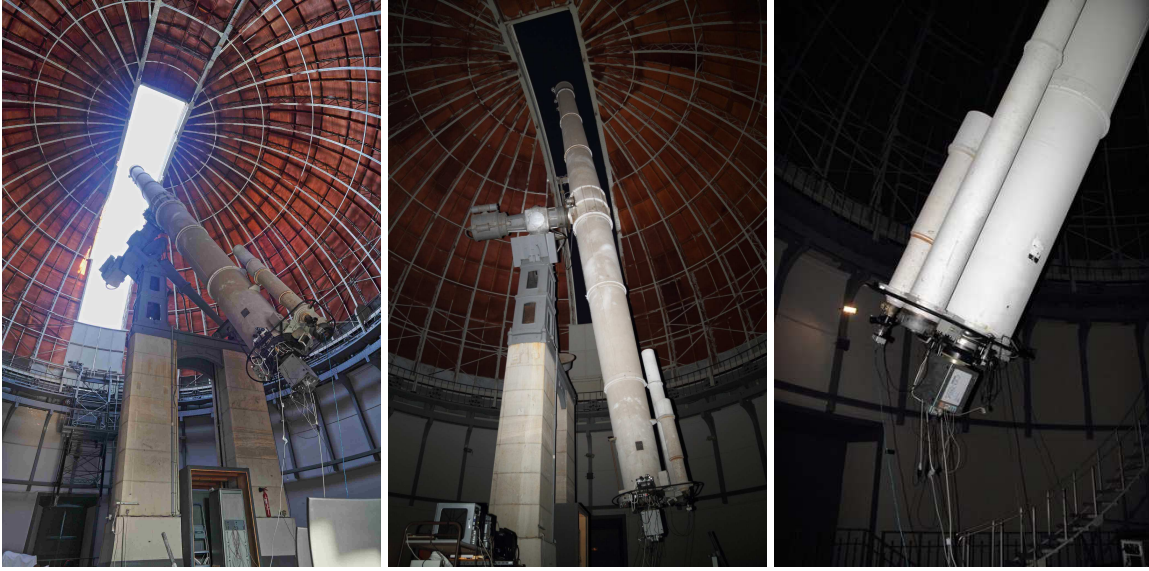


Figure 1: PISCO2 on the Nice 76-cm refractor (L76). The largest finder which is mounted on “piggy-back” is a Zeiss 25-cm refractor.

The optical design of PISCO2 is similar to that of PISCO but the observing modes are reduced, and are mainly limited to speckle observations. Indeed, PISCO2 was specially designed for the observation of visual binary stars. Associated with an electronic detector, it allows the acquisition of enlarged short exposure images exhibiting “speckles”. Those images can then be processed as first suggested by Labeyrie (1970), to provide high-angular resolution information.

In this paper, we first present the L76 refractor (Sect. 2) and the modifications we have done to make it fully operational. The instrumental setup of PISCO2 and its main technical capabilities are described in Sect. 3. The atmospheric-dispersion corrector which is using Risley prisms is presented in Sect. 4. The absolute scale calibration of PISCO2 can be done with a grating mask placed on the entrance pupil of the telescope. The whole calibration procedure is explained in Sect. 5.

2 The Nice 76-cm refractor

PISCO2 was specially designed for the Nice 76-cm refractor belonging to Observatoire de la Côte d’Azur (OCA). Built in 1887, when it was the largest refractor in the world, this famous telescope has a free aperture diameter of $D = 74$ cm and a focal length of 17.89 m (see Fig. 1). It is one of the largest refractors still in operation in the world. It has mainly been devoted to binary observation since its construction. The good quality of its optics makes Airy rings clearly visible when the seeing is good. And this happens very frequently, despite the vicinity to Nice city.

Paul Couteau is probably the most famous astronomer who has used it. He was the architect of the renovation of this refractor from 1965 to 1969 (Couteau, 1970) and many binaries of his impressive Couteau’s catalogue (Couteau, 1993), were measured with this telescope (e.g., Couteau & Gili, 1994, Gili & Couteau, 1997). When he retired in 2000, one of his closest collaborators, R. Gili (hereafter RG), decided to continue this long story of binary observations with the L76. Although he was an experimented binary star observer with a filar micrometer, RG wanted to use more



Figure 2: Webcams used for reading the hour angle (H.A.) and declination (Dec.) circles and thus allowing remote control of the L76 refractor. Left panel: H.A. webcam, central panel: Dec. webcam, upper right panel: Horloge program (from G. Morlet), lower right panel: webcam images of the H.A. and Dec. circles.

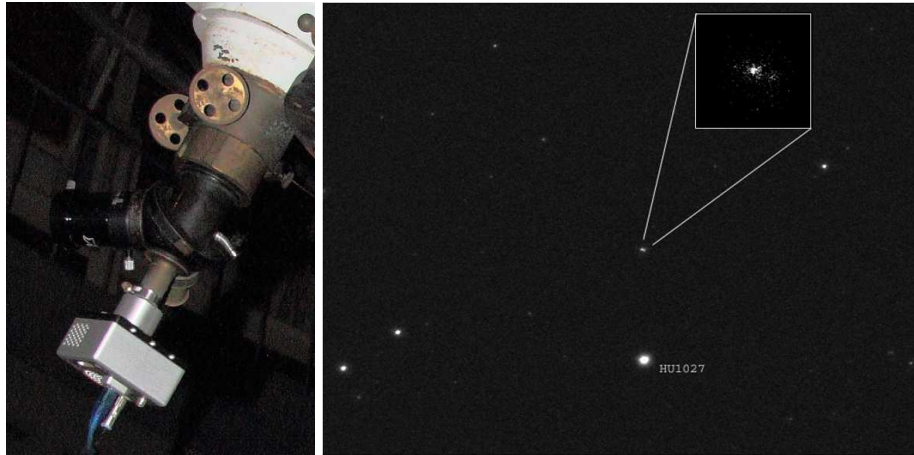


Figure 3: ANDOR LUCAs camera at the focus of the Zeiss refractor (left) which is used as a wide-field finder for speckle observations with the L76 refractor. Right: comparison of the corresponding field of view ($9' \times 12'$) with that provided by the ANDOR DV885 camera on the L76 ($16'' \times 16''$).

modern techniques, like precise binary measurements on short-exposed CCD (Charge-Coupled Device) images that he had already obtained in collaboration with other colleagues (Salaman et al., 1999, Morlet et al., 1999, 2002, Gili & Bonneau, 2001). For this new operating mode, it soon appeared that the L76 needed a serious revision and that a specially designed speckle camera was needed for improving the efficiency and quality of those observations. The 76-cm lens was then dismantled, thoroughly cleaned, and the two (crown and flint) components were fitted into a new improved mechanical mount. The dome motorisation was thoroughly revised, both for the electronics and the mechanics.

In 2008, two webcams were fitted to the existing magnifying optics of the hour angle and declination circles to allow their reading from a dedicated control computer (Fig. 2). This allowed the observer to safely control the telescope while remaining seated in front of a control computer. Before this modification, for pointing any object with the telescope, the observer had to move to each of the two coordinates circles and then climb on top of a ladder to watch the star in the finder. Obviously, this could be dangerous in the darkness, especially when the observer started to be tired and feeling sleepy (!). Due to the large size of the telescope (about 18 m), this was very particularly dangerous when the telescope was pointing to low elevation targets. A few months later, a new ANDOR DV885 camera was acquired for speckle observations, and replaced the ANDOR LUCAs that was formerly used for this task. This ANDOR LUCAs camera was installed on the Zeiss 25 cm finder, and was thus able to transmit field images to the control computer (see Fig. 3). This happened to be a decisive improvement to the pointing procedure, since from then both the L76 telescope and its focal instrumentation could be operated from this computer, by a single observer.

Focusing the telescope was another hazardous operation, especially for observations done by a single observer (by far the most frequent case). For CCD or EMCCD observations, the observer had to climb on the top of a large step-ladder to actuate the big focusing hand-wheel, then go down for checking the quality of the CCD image on the computer screen. This had to be done a few times until satisfactory focusing was achieved. Furthermore, this operation had to be done in full darkness, which was needed to avoid saturating the camera.

The few thousands of measurements published in Gili & Agati (2009) and Gili & Prieur (2012) were obtained in those difficult conditions. Indeed, the original focusing system was part of the L76 mechanics and could not be motorized easily, without a thorough modification of this historical instrument. Consequently, an important specification for the design of PISCO2 was to include a remote control focusing capability.

3 Presentation of PISCO2

The decision to build a new speckle camera for the L76 was taken in 2009. The main idea was to ease and speed up the observations while extending the observable domain to lower elevation targets. The basic constraints were: simplicity, lightness, small overall dimensions, and low cost. The last constraint was rather severe since most of the expenditure had to be covered by personal funds. For this design, we took profit of our experience in binary star observations with the L76 and with PISCO on other telescopes.

PISCO2 was entirely made at OCA between 2010 and 2012 (see Figs. 4, 5). Most of the mechanical parts were machined in the OCA workshops. When possible complete manufactured units were integrated into PISCO2, to reduce the development time and the cost. For example, this was the case for the remote-control units dedicated to the motorized focusing or the angular control of the Risley prisms (see Fig. 6).

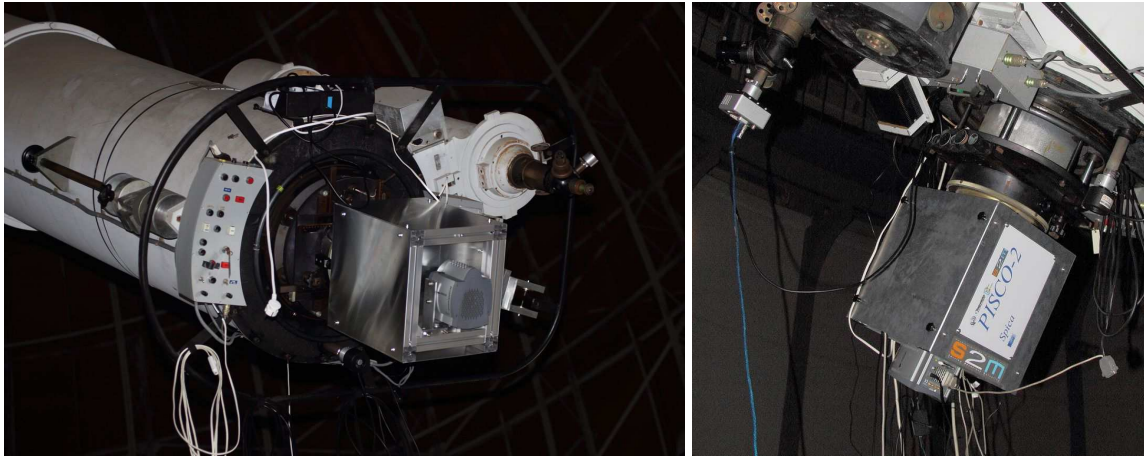


Figure 4: PISCO2 with the ANDOR DV897 EMCCD camera at the focus of the 76-cm refractor.

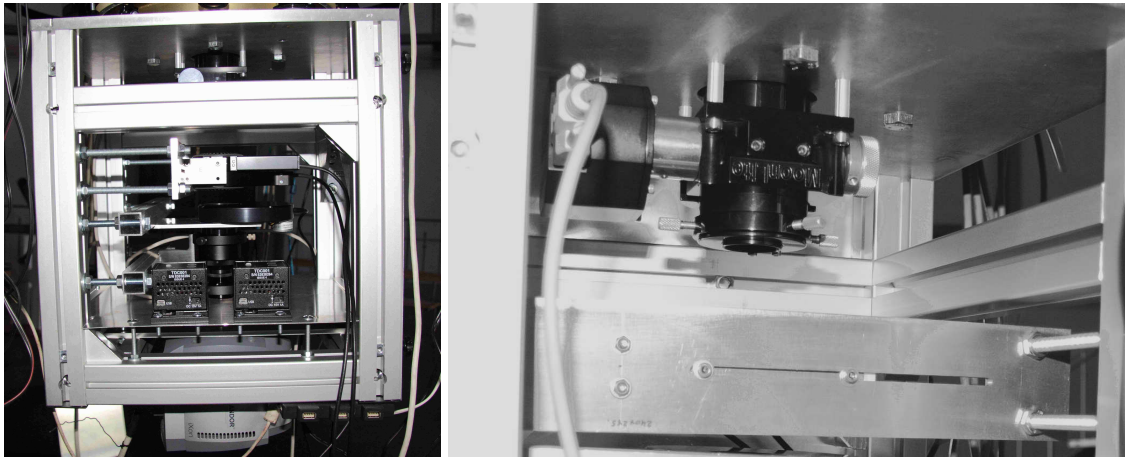


Figure 5: PISCO2: inside views. Left: general overview. The remote controlled Risley prisms and the two corresponding USB-interface boxes are located at the bottom of this image. Right: close up view of the motorized focusing system.



Figure 6: PISCO2: remote control of the Risley prisms (left panel), motorized focusing (central panel) and filter wheel selection (right panel).

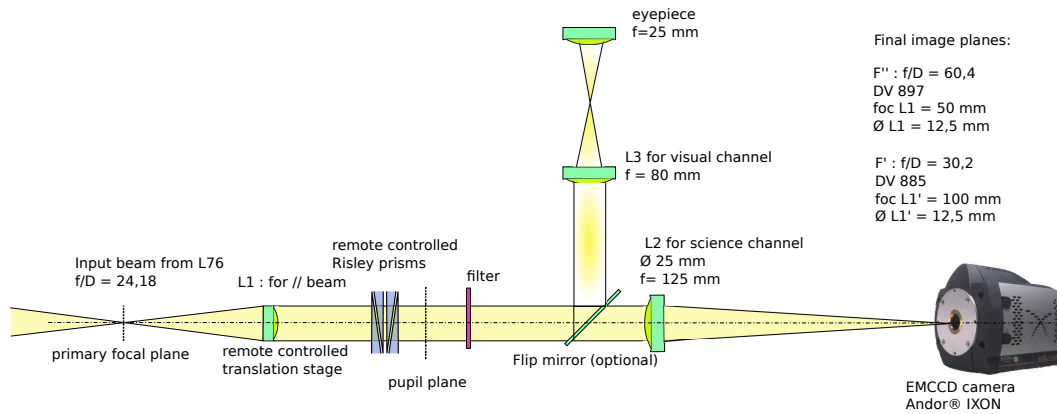


Figure 7: PISCO2: optical layout.

3.1 Optical design

The optical layout (see Fig. 7) is similar to that of PISCO (see Prieur et al., 1998). An achromatic lens L1 of focal length F_1 is placed at a distance F_1 from the primary focus plane of the telescope. This lens thus creates a collimated beam which is used for placing the Risley prisms and the filters. A second achromatic lens L2 focuses this parallel beam onto the image plane of the detector. A retractable mirror and a set of two lenses (L3 and eyepiece) enable a visual inspection of the images. The Risley prisms are located very close to the pupil plane. Contrarily to PISCO, there is no field lens in the focal plane of the telescope. This improves the overall transmission, but imposes a longer distance for the collimated beam.

PISCO2 can use different detectors, which may have different pixel sizes. The adaptation can be done by changing the lens L1, and choosing its focal length value accordingly. For instance, two L1 lenses of 50 and 100 mm focal length have been used for the ANDOR DV897 and DV885 detectors, respectively.

The available filters are:

- the IRC (IR-cut), which is a lower-pass filter rejecting all wavelengths above 700 nm;
- the Schott BG39, which is a band-pass between 350 and 600 nm;
- and the AF (anti-fringe or V-block), which is a bandpass 450–650 nm;

The AF filter considerably reduces the secondary spectrum of the 76-cm refractor, with no significant loss of energy in the V band. When combined with the transmission of the lenses and the quantum efficiency response of the detector, the resulting transmission curve of those filters is close to a standard V filter with a maximum around 570 nm.

Most optical settings of PISCO2 can be remotely controlled with a computer:

- Focusing
- Filter selection
- Risley prism correction

Motorised focusing and filter wheel selection are controlled by ASCOM interface programs provided by the corresponding manufacturers. Focusing is driven by a step motor whose step corresponds to a translation of $4\mu\text{m}$, with a full range of 40 mm. Risley prisms can be set by the THORLABS program which works with a USB interface (see Fig. 6).

Table 1: Main characteristics of the ANDOR iXON EMCCD cameras used for our observations. The quantum efficiency in Col. 6 is the value given by the manufacturer for the EMCCD chip. The overall effective efficiency is much smaller.

Name	Format (pixels)	Pixel size (μm)	Digitization (bits)	Read freq. (MHz)	Quantum Eff. (%)	Max. cooling T. ($^{\circ}\text{C}$)
DV885	1004×1002	8×8	14	27	60-65	-70
DV897	512×512	16×16	14	10	80-92	-90

3.2 Description of the detectors

The PISCO2 instrument was successively fitted with two EMCCD detectors from ANDOR Technology: an iXON DV885 and an iXON DV897 (see ANDOR, 2014). We first used the DV885 belonging to RG, that is equipped with a front-illuminated EMCCD chip. We then used the DV897 belonging to F. Vakili (FV), which is more recent and has better performances. It has a back-illuminated EMCCD with a higher quantum efficiency and is fitted with a more elaborated cooling system. Another advantage of the DV897 is its higher reading frequency.

The main characteristics of the two detectors are given in Table 1. For each one, we indicate its full format in pixels (Col. 2), the pixel size in μm (Col. 3), the digitization depth in Col. 4, i.e. the number of bits per pixels used for encoding the output values, the maximum frequency rate (Col. 5) used for reading out the pixel data, the theoretical quantum efficiency of the detector (Col. 6), and the cooling temperature that was used during our observations (Col. 7).

The quantum efficiency values in Col. 6 of Table 1 are those given by the EMCCD chip constructor for wavelengths in the range 550–720 nm. The overall effective efficiency is unfortunately much smaller. With PISCO in Merate (Italy), we have done some comparative tests in 2011 with the iXON DV885 and the PISCO ICCD cameras (see Scardia et al., 2013). For speckle observations, the DV885 was roughly equivalent to the ICCD. Note that the ICCD camera is fitted with a R-photo-cathode amplifier whose quantum efficiency is 7% only (!).

For both detectors, the image transfer is done through a dedicated link between the detector and a CCI-22 frame grabber board installed on a PCI slot of the acquisition computer, which allows a reading frequency as high as 27 MHz. This would correspond to an acquisition rate of 27 full-size images per second. In practice, we used a lower readout frequency (5.13 MHz) to reduce the noise in the images. Those detectors can be used in EM mode, which reduces the read-out-noise of the output register to less than one electron.

We wrote a specially designed program (buildspeck1) for handling the data acquisition of those two detectors (see Fig. 8). This program controls the electronic settings and the basic functions of the EMCCD detectors. It also performs real-time processing of speckle interferometry observations.

Exposure times of elementary frames are set in the range 20–30 msec for speckle observations. The standard format of the acquisition window is 128×128 pixels which corresponds to a field of view of $9.5'' \times 9.5''$ for the DV897 camera. For faint objects or wide pairs, a wider field of 256×256 pixels on the detector can be used with a binning factor of 2×2 which thus amounts to 128×128 pixels for the elementary frames. The EM gain is generally set to values of about 170–200 and

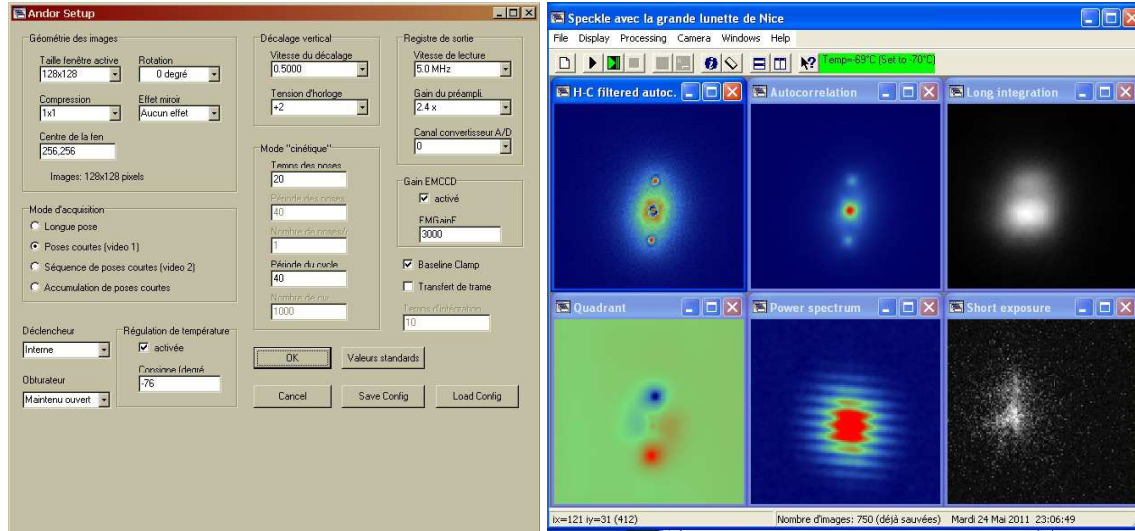


Figure 8: Program buildspeck1 used for data acquisition with ANDOR cameras and real-time processing. Left: camera setup; right: example of image processing of the binary star BU 1273 ($\rho = 1.''3$, $m_V = 9.6$ $\Delta m_V = 1.3$).

3000 for the DV885 and the DV897, respectively. To avoid saturation with bright objects, the EM gain can be reduced or even put to “off”, which corresponds to observing in conventional CCD mode.

4 Correction of the atmospheric dispersion with Risley prisms

For ground-based observations of astronomical objects, the atmosphere behaves like a dispersive prism (see f.i., Simon, 1966). Polychromatic images are spread into a small vertical spectrum. This effect can be neglected for observations close to the zenith, but is very strong at low elevations, and can severely degrade the angular resolution. For instance in the visible, for a $\Delta\lambda = 250$ nm bandpass centered at $\lambda = 500$ nm, the typical atmospheric dispersion is $\Delta\theta = 1''$ for an elevation $h = 60^\circ$ and $\Delta\theta = 2''$ for $h = 30^\circ$.

PISCO2 contains an atmospheric dispersion corrector to circumvent this problem. This corrector is similar to that of PISCO (see Prieur et al., 1998) and is based on “Risley prisms” (see f.i. Breckinridge *et al.* 1979, Walner & Wetherell, 1990). They consist in two identical sets of prisms that can be rotated to produce a tunable chromatic dispersion both in amplitude and direction. Each set is made of two prisms that have different indices and roof angles, and that are glued together in an upside-down position (see Fig. 9).

Like for PISCO, we have used the same combination of Schott glasses (F4, SK10) which was also used for the Kitt Peak speckle camera (Breckinridge *et al.*, 1979). There are of course other possibilities, like the combinations proposed by Wallner & Wetherel (1990), which are closer to the atmospheric dispersion curve. The F4+SK10 combination has the advantage of a low cost and was sufficiently efficient for our purpose.

The Risley prisms of PISCO2 have been designed to have a null mean deviation, and a dispersion allowing atmospheric correction from the zenith down to an elevation of 30° , when using the DV897 detector. The F4 and SK10 prisms have a roof angle of 10.0° and 9.92° respectively. The

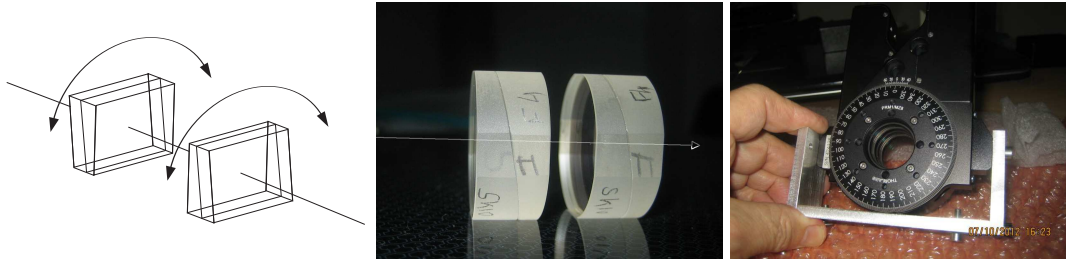


Figure 9: PISCO2 Risley prisms used for atmospheric dispersion correction. From left to right: schematic drawing, view of the prisms, and THORLABS motorized wheel

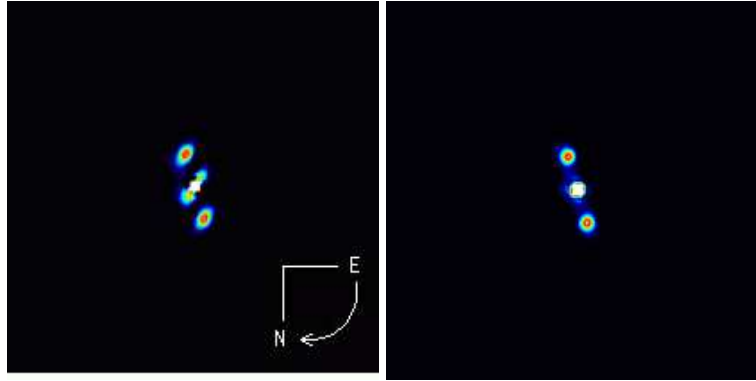


Figure 10: Effect of the atmospheric dispersion on the autocorrelation of a binary star (left) and correction with Risley prisms (right). Object: A2724, $\rho = 0.''8$, $\theta = 197^\circ$, $m_V = 8.4$, $\Delta m_V = 0.7$, observed at a zenith distance of $z = 42^\circ$.

tolerance on the roof angle is 6 arcmin, and the surface accuracy is $\lambda/4$ (for $\lambda=550$ nm). Those specifications lead to a reduction of the residual dispersion down to a level smaller than 0.01" for any object located at an elevation larger than 30° , with the AF filter (450-650 nm bandpass). This value is much smaller than the diffraction limit of 0.16" of the 76-cm refractor.

During the observations, a specially designed program (`pisco2_risley.cpp`) computes the elevation of the star and the atmospheric dispersion inferred from models (Owens, 1967, formulae 29–31). The Risley prisms are then rotated with the THORLABS remote-control program, so that their total dispersion has the same magnitude as the atmospheric dispersion and an opposite direction. The observations have shown that the correction is very good, even for objects whose declination is as low as -7° , which is the pointing lower limit for the present instrumentation setup, due to the camera cable length. (see Figs. 10, 11).

5 Scale calibration with a grating mask

The on-sky pixel scale of the whole instrument (telescope and PISCO2) can be calibrated in an absolute manner with a grating mask placed in front of the refractor objective lens. This is the method used for calibrating PISCO in Merate, as described in detail in Scardia et al. (2007). We present here the procedure we followed in September 2012 for calibrating the scale of the DV897 detector.

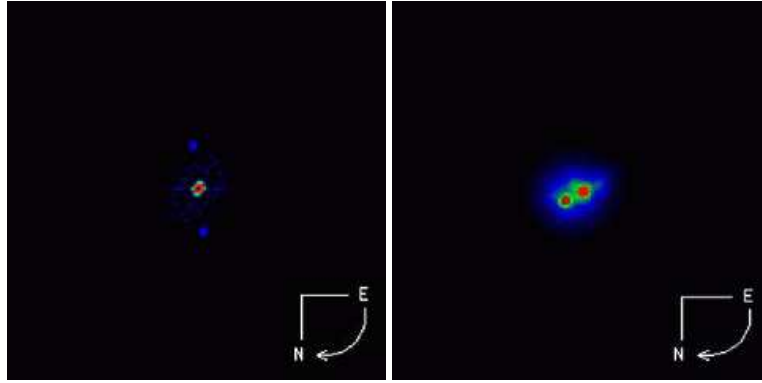


Figure 11: Left: mean autocorrelation of RST 4712 ($m_V = 9.8$, $\Delta m_V = 1.2$, $\rho = 1.''1$, $\theta = 193^\circ$). Right: image obtained by adding recentered selected images (Lucky imaging) of STF 2696 ($m_V = 7.9$, $\Delta m_V = 0.8$, $\rho = 0.''5$, $\theta = 298^\circ$). Due to the large zenith distance of those observations (50° and 40° , respectively) Risley correction was needed (and successfully applied) in both cases.

As shown in Fig. 12, a grating mask was mounted on the entrance baffle of the telescope. This mask was originally designed for the calibration of the OCA 50-cm refractor. It has a diameter of 50 cm and a period of 22.43 ± 0.10 mm. To obtain measurements with a high precision, we used a narrow-band filter, centered on $\lambda = 570$ nm, with a bandwidth of $\Delta\lambda = 10$ nm. The corresponding period of the diffraction pattern was then $\lambda/p = 5''.241$. For this calibration, we observed the single star ϵ Leo. The measurements were made on the mean of a series of a few 1000-image data cubes. The equivalent focal length with PISCO2 and the DV897 detector was found to be $F = 44.66 \pm 0.2$ m and the scale of $0.0739''/\text{pixel}$.

The 76-cm refractor has actually a free aperture of 74 cm. The corresponding limit of diffraction $\rho_D = \lambda/D$ is $0''.16$ with $\lambda = 570$ nm. The sampling of this detector mounted on PISCO2 is thus smaller than $\rho_D/2$ for $\lambda = 570$ nm. This sampling is compatible with the Nyquist-Shannon criterion, and therefore allows measurements down to the telescope diffraction limit.

The calibration of the origin of the position angles was done recording star trails caused by the diurnal motion. We used the largest available field for this purpose, which was $53'' \times 40''$ with the DV897.

6 Conclusion

The first observations have shown that PISCO2 performances have reached the initial goal. Fitted with remote-control components such as a filter wheel, a motorized focusing system, and an atmospheric dispersion corrector, this instrument is very easy to operate.

PISCO2 is dedicated to the observation of visual binary stars. In the last few years, it has already permitted to obtain numerous measurements, with a average rate of about 2100 objects/yr. With the DV897 detector, we have been able to observe faint close binary stars with angular separations as small as $0''.16$, and visual magnitudes of about 16. We also have measured some particularly difficult systems with a magnitude difference between the two components of about 4 mag.

Those performances are very promising for the detection and study of large sets of yet unknown (or partly measured) binaries with close separation and/or large magnitude difference, many of which could not be measured by space missions. PISCO2 may thus provide a significant contribution to stellar physics.

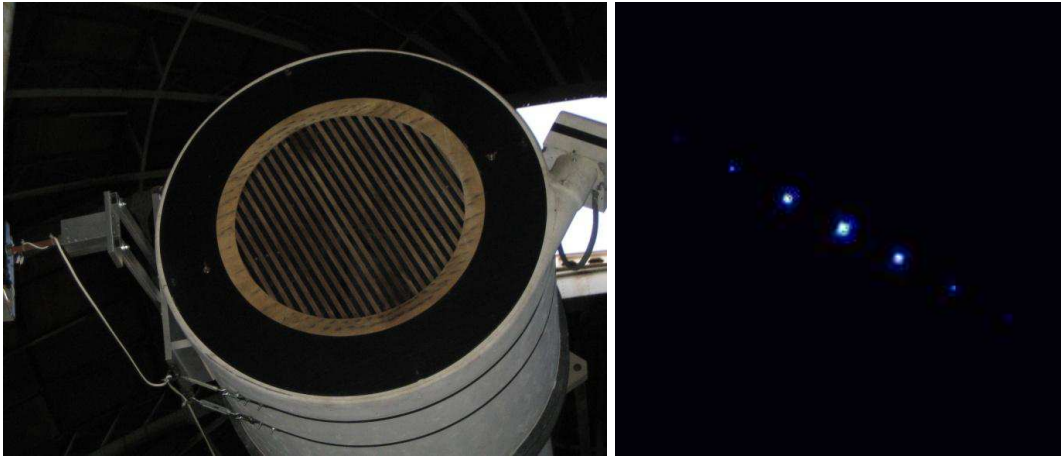


Figure 12: Scale calibration with a grating mask. Left: mask placed on top of the 76cm-refractor. Right: mean autocorrelation of the diffraction pattern obtained with ϵ Leo.

Acknowledgements

We are indebted to the direction of Observatoire de la Côte d'Azur for allowing us to use the 76-cm refractor. We thank the workshop staff of this observatory for their technical support and Y. Bresson (OCA) for his contribution to the optical design of PISCO2. We are also very grateful to R.W. Argyle (Cambridge, U.K.) for checking the English of this paper.

References

- [ANDOR(2014)] ANDOR: 2014, ANDOR technology <http://www.andor-tech.com>
- [Breckinridge et al.(1979)] **Kitt Peak speckle camera**
Breckinridge, J.B., McAlister, H.A., Robinson, W.G., 1979, Appl. Optics, 18, 7, 1034–1041.
- [Couteau (1970)] **La grande lunette de l'Observatoire de Nice**
Couteau, P., 1970, L'Astronomie, 84, 213
- [Couteau (1993)] **Catalogue de 2700 étoiles doubles**
Couteau, P., 1993, Obs. Côte d'Azur, Nice, 2nd Edition.
- [Couteau & Gili (1994)] **Mesures d'étoiles doubles faites à Nice, étoiles doubles nouvelles (24ème série) découvertes à Nice.**
Couteau, P., Gili, R., 1994, A&AS, 106, 377
- [Couteau & Gili (1997)] **Mesures d'étoiles doubles faites aux lunettes de 74 et 50 cm de l'Observatoire de la Côte d'Azur.**
Gili, R., Couteau, P., 1997, A&AS, 126, 1
- [Gili & Bonneau (2001)] **CCD measurements of visual double stars made with the 74 cm and 50 cm refractors of the Nice Observatory (2nd series)**
Gili, R., Bonneau, D., 2001, A&A, 378, 954

- [Gili & Agati(2009)] **Measurements of double stars with the 76 cm refractor of the Côte d’Azur observatory with CCD and emCCD cameras. 2nd part.**
Gili, R., Agati, J.-L., 2009, *Observations & Travaux*, 74, 14
- [Gili & Prieur(2012)] **Relative astrometric and photometric measurements of visual binaries made with the Nice 76-cm refractor in 2008**
Gili, R., Prieur, J.-L., 2012, *Astron. Nach.*, 333, 727–735
- [Labeyrie(1970)] **Attainment of diffraction limited resolution in large telescopes by Fourier analysing speckle patterns in star images**
Labeyrie A.: 1970, *A&A*, 6, 85
- [Morlet et al.(1999)] **CCD measurements of visual double stars made with the 50 cm refractor of the Nice Observatory (2nd series)**
Morlet, G., Salaman, M., Gili, R., 1999, *A&AS*, 135, 499
- [Morlet et al.(2002)] **Nice Observatory CCD measurements of visual double stars (4th series)**
Morlet, G., Salaman, M., Gili, R., 2002, *A&A*, 396, 933
- [Owens(1967)] **Optical refractive index of air: dependence on pressure, temperature and composition**
Owens, J.C., 1967, *Applied Optics*, Vol. 6, N°1., 51–59.
- [Prieur et al.(1998)] **The PISCO speckle camera at Pic du Midi Observatory**
Prieur, J.-L., Koechlin, L., André, C., Gallou, G., Lucuix, C.: 1998, *Experimental Astronomy*, vol 8, Issue 4, 297
- [Salaman et al.(1999)] **CCD measurements of visual double stars made with the 50 cm refractor of the Nice Observatory**
Salaman, M., Morlet, G., Gili, R., 1999, *A&AS*, 135, 499
- [Scardia et al.(2007)] **Speckle observations with PISCO in Merate. III. Astrometric measurements of visual binaries in 2005 and scale calibration with a grating mask**
Scardia M., Prieur J.-L., Pansecchi L., Argyle R.W., Basso S., Sala M., Ghigo M., Koechlin L., Aristidi E., 2007, *MNRAS*, 374, 965–978
- [Scardia et al.(2013)] **Speckle observations with PISCO in Merate. XII. Astrometric measurements of visual binaries in 2011**
Scardia, M., Prieur, J.-L., M., Pansecchi, L., Argyle, R.W., Spanó, P., Riva, M., Landoni, M., 2013, *MNRAS*, 434, 2803–2813
- [Simon(1966)] **A practical solution of the atmospheric dispersion problem,**
Simon, G.W., 1966, *Astron. J.*, 71, 190.
- [Wallner & Wetherell(1990)] Wallner, E.P., Wetherell, W.B., 1990, *Broad spectral bandpass atmospheric dispersion correctors*, Rapport technique Itek.